The 2020 Beirut Explosion:

Simplified Warehouse Fire Analysis

for Forensic Architecture

February 12, 2023

Authored by Antonio Cicione & Danielle Antonellis

Table of Contents

Disclaimer

Kindling understands that this report will be made available to Forensic Architecture as input to their investigation of the warehouse fire and explosion on 4 August 2020 in the port of Beirut, Lebanon. The analysis undertaken in this report is based solely on images, data and parameters provided by Forensic Architecture, and does not reflect a fully independent investigation of the available data and information that might otherwise be available.

Executive Summary

Forensic Architecture is carrying out an investigation of the 4 August 2020 fire and explosion which ripped through the port of Beirut, Lebanon. This incident killed more than two hundred people, wounded over 6500, and destroyed large parts of the city. Forensic Architecture was invited by Mada Masr to examine open-source information including videos, photographs, and documents and to provide a timeline of the incident and a detailed 3D model to help investigate the events of that day. In support of this request, and in pursuit of political and economic accountability, Forensic Architecture made their model, the geolocated videos and the source material used in their research, publicly available here: *https://forensic-architecture.org/investigation/beirut-port-explosion*

As an input to their investigation, Forensic Architecture requested Kindling carry to out an analysis of the warehouse fire that evidently led to the explosion of ammonium nitrate. Forensic Architecture had a very specific question for Kindling to respond to:

Which of the two areas depicted in Figure 3, identified by Forensic Architecture, is the most likely region of fire origin, based on information provided?

- P1, the location previously identified by Forensic Architecture [1] as the source of the smoke plume leaving the warehouse during the early stages of the fire; or
- P2, a new location of interest based on known welding activities that occurred earlier on the day of the incident.

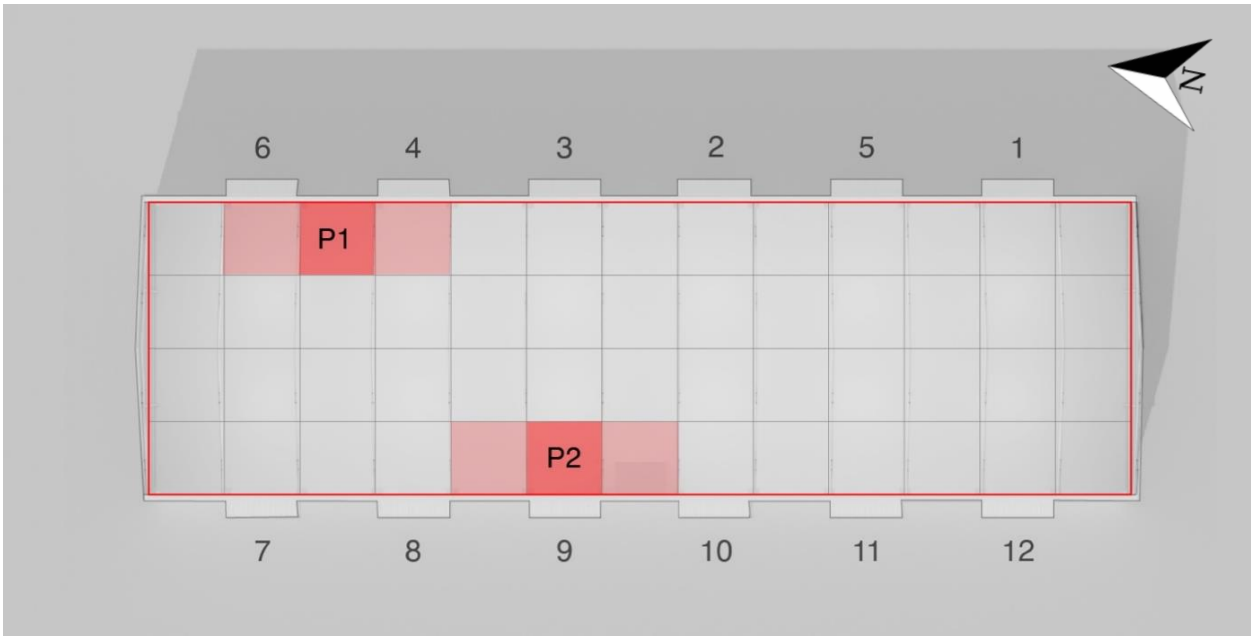

Figure 1: Two areas of interest, © forensic architecture

In this regard, Kindling's work is not an investigation, but an analysis of scenarios identified by Forensic Architecture. In conducting this analysis, Kindling relied solely on

information provided by Forensic Architecture for this simplified analysis and responded only to the question posed by Forensic Architecture above.

Since very little information was available about the type and distribution of fuel in the warehouse and potential ignition sources, potential fire scenarios were not identified or evaluated. Rather, this simplified analysis aims to identify the more likely region of fire origin between only regions P1 and P2, identified by Forensic Architecture, by analyzing an externally observable sequence of events from video footage, i.e., smoke behavior, flame extensions, and melting of roof vents. Utilizing video footage and information provided by Forensic Architecture, on ventilation conditions Kindling used computational fluid dynamics (CFD) modelling to identify the most plausible region of fire origin between region P1 and P2.

In this report, the fire analysis methodology, CFD results, and relevant findings are presented and discussed. The most likely region of fire origin between the two locations in question has been identified as P1, based on the information provided by Forensic Architecture. The main findings are as follow:

- By analysing external smoke plume patterns and the location of melted vents, it was determined that the most likely source of heat was located in the northeast corner of Warehouse 12.
- For the P1 numerical simulations, based on the assumptions made regarding the fuel load and distribution, it was shown that the open vents in the P1 numerical scenarios correlated well with those identified in the video analysis. Whereas, for the P2 numerical simulations, the open vents in the numerical scenarios did not correlate well with those identified in the video analysis.
- Comparing the smoke patterns and areas where the smoke left Warehouse 12 for scenario P1 and P2 to the actual event, it is observed that the P1 modelling results correlated well with video evidence of the actual event, whereas P2 scenarios and actual event did not correlate well.

Hence, based on the analyses undertaken in this work, and the information available at the time of the analysis, location P1 is proposed as the most likely region of fire origin between the two regions, P1 and P2, identified by Forensic Architecture.

1 Introduction

Forensic Architecture is carrying out an investigation of the 4 August 2020 fire and explosion which ripped through the port of Beirut, Lebanon. This incident killed more than two hundred people, wounded over 6500, and destroyed large parts of the city. Forensic Architecture was invited by Mada Masr to examine open-source information including videos, photographs, and documents and to provide a timeline of the incident and a detailed 3D model to help investigate the events of that day. In support of this request, and in pursuit of political and economic accountability, Forensic Architecture made their model, the geolocated videos and the source material used in their research, publicly available here: https://forensic-architecture.org/investigation/beirut-port-explosion

Warehouse 12, the origin of the explosion, was located at the Beirut port in Lebanon next to the grain silos as depicted in Figure 2.

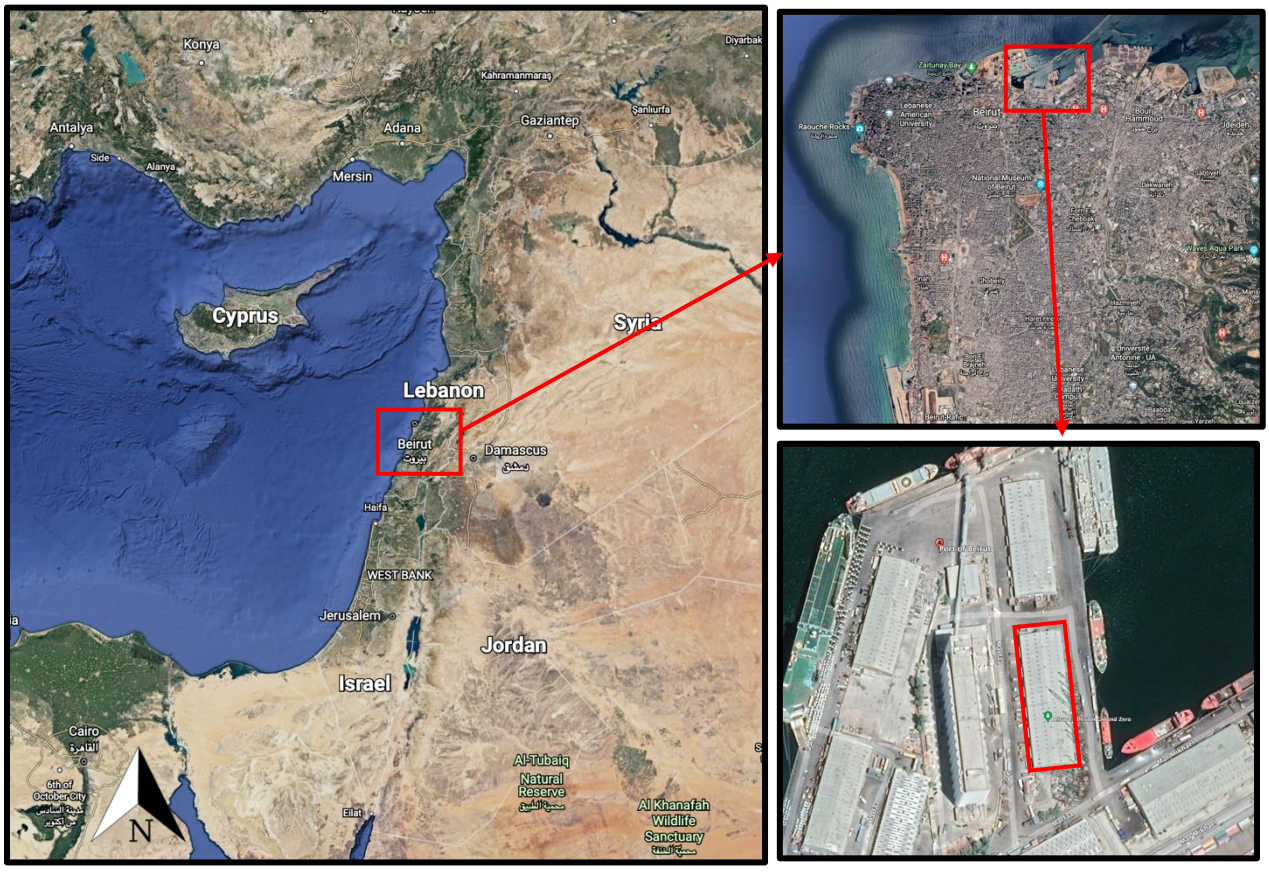

Figure 2: Location of Warehouse 12 based on Google Earth Imagery

A summary of the timeline provided by Forensic Architecture's previous work is shown in Table 1. A more detailed discussion pertaining to the incident is provided in ref [1].

Table 1: Summary of the Beirut port explosion fire incident timeline [1]

Time	Description
15h30	Workers leave the premises
17h54	Fire first tweeted
17h55	Security informs the fire brigade of a blaze at the port
17h55	First video footage of the incident
18h04	The fire brigade arrives at the scene
18h07	Fireworks explosion
18h08	Ammonium nitrate explosion

As an input to their investigation, Forensic Architecture requested Kindling to carry out an analysis of the warehouse fire that evidently led to the explosion of ammonium nitrate. Forensic Architecture had a very specific question for Kindling to respond to:

Which of the two areas depicted in Figure 3, identified by Forensic Architecture, is the most likely region of fire origin, based on information provided?

a) P1, the location previously identified by Forensic Architecture [1] as the source of the smoke plume leaving the warehouse during the early stages of the fire; or
b) P2, a new location of interest based on known welding activities that occurred earlier on the day of the incident.

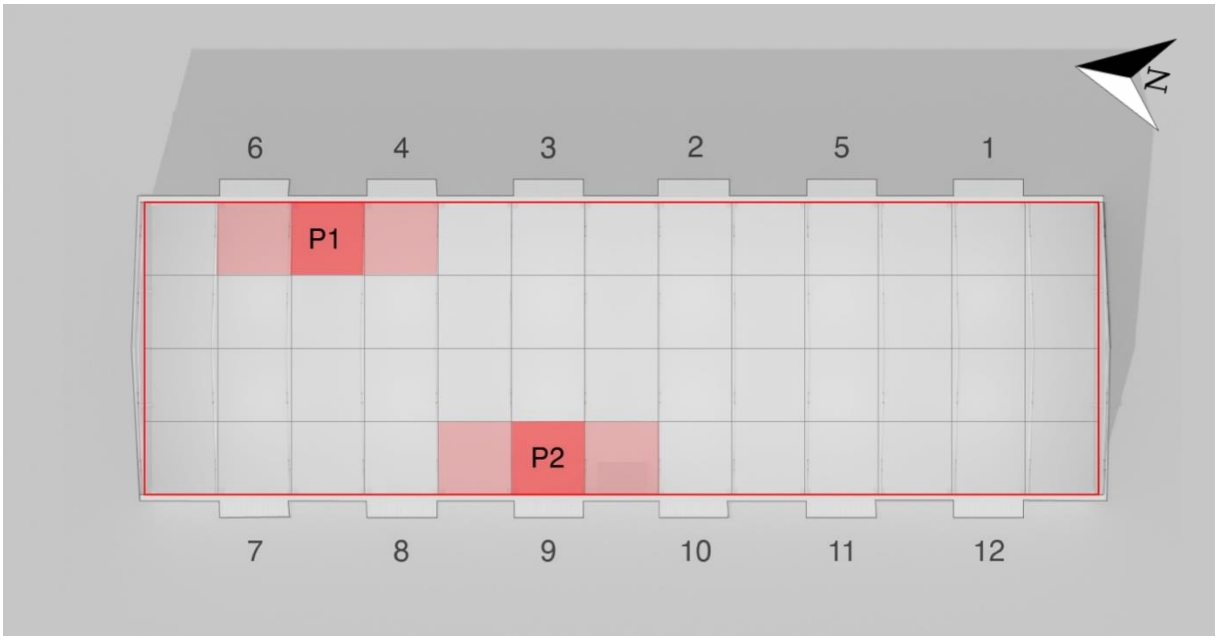

Figure 3: Two areas of interest, © forensic architecture

Kindling's work is not an investigation. Kindling relied solely on the information provided by Forensic Architecture for this simplified analysis and responded only to the question posed by Forensic Architecture above.

Very little information was available about the type and distribution of fuel in the warehouse and potential ignition sources. Therefore, potential fire scenarios were not identified or evaluated. Rather, this simplified analysis aims to identify the more likely region of fire origin between only regions P1 and P2 by analyzing an externally observable sequence of events from video footage, i.e., smoke behavior, flame extensions, and melting of roof vents. Utilizing video footage and information provided by Forensic Architecture, on ventilation conditions Kindling used computational fluid dynamics (CFD) modelling to identify the most plausible region of fire origin between region P1 and P2.

The purpose of this report is to share Kindling's fire analysis methodology, CFD results, and relevant findings. It does not address any items for which specific information has not been provided, or questions beyond the question from Forensic Architecture outlined above.

2 Goal and objectives

The goal of this work is to share a simplified fire analysis regarding the more plausible region of fire origin, between locations P1 and P2 identified by Forensic Architecture within Warehouse 12 located at the port of Beirut, Lebanon. To achieve this goal, the objective of this work is to analyze information provided by Forensic Architecture pertaining to the predefined regions of potential fire origin, P1 and P2, including the externally observable sequence of events from video footage, i.e., smoke behavior, flame extensions, and melting of roof vents, and comparing this footage to the results of CFD scenarios.

3 Limitations

As a result of the complexity of this fire incident, lack of data (e.g., unknown fuel load and distribution in the warehouse), scope limitations (i.e., only considering the two proposed fire origin regions by Forensic Architecture), and time constraints, only a limited number of numerical models were conducted in this work and thus, the results should be interpreted accordingly. The following are limitations or exclusions of the work presented in this report:

- Kindling's work is not an investigation. Kindling relied solely on information provided by Forensic Architecture for this simplified analysis and responds to the specific question posed by Forensic Architecture.
- This simplified analysis does not consider other potential ignition regions or specific fire scenarios. Without additional information and a full investigation, Kindling acknowledges it is possible that the fire could have originated in a different region of the warehouse than proposed herein.
- It is Kindling's understanding that insufficient information is available to identify the precise cause, location, and sequence of the fire incident due to the severity of

damage at the scene of the fire and explosion. Regardless, this falls outside the scope of Kindling's work as described above.

- This works only considers the fire that led to the explosion and not the explosion itself.
- The warehouse construction materials and fuel conditions were not available to Kindling. Therefore, many assumptions were made regarding the simplified fire scenarios used for modelling purposes.
- Detailed Fire Dynamics Simulator (a fire and smoke modelling software) analyses could not be performed due to a lack of information about the fuel load, materials, and conditions within the warehouse. Computational limitations and time constraints further motivated a simplified approach. The results should be interpreted accordingly.

4 Overview of warehouse and content

Figure 4 depicts the orientation of Warehouse 12. The prevailing wind direction is also indicated on Figure 4 (blue arrow), with more detailed wind directions and speeds listed in Table 2, as provided by Forensic Architecture. The ambient temperature during the time of the fire incident was approximately 30 ºC [1].

Figure 4: Orientation of Warehouse 12. Prevailing wind directions depicted with a blue arrow

The grain silos and the other warehouse, located to the west and north of Warehouse 12, are located approximately 45 m and 35 m from Warehouse 12, respectively. Warehouse 12 has a floor area of 5330 m^2, and the height from the ground to the apex of the duo-pitched roof (12 degrees slope) is approximately 14 m.

Table 2: Summary of wind speeds and directions during the fire incident provided by Forensic Architecture.

Time	Direction	Speed [m/s]
15h00	SW	7.2
16h00	WSW	6.3
17h00	WSW	5.8
18h00	WSW	5.8
19h00	SW	5.3

Warehouse 12 was clad with steel sheets (the exact sheet type used is unknown), as depicted in Figure 5. The roof had several equally spaced opaque plastic panels for skylights (the exact material of the plastic sheets is unknown but is most likely polycarbonate-type or PVC-type sheets, based on visual observations), as depicted in Figure 5. The long walls (east and west walls) of Warehouse 12 had two rows of windows spanning the length of the building. Some of these windows appeared to be open prior to the fire incident based on video analysis. The windows were incorporated in the 3D models created by Forensic Architecture [1] with observed open/closed status.

Figure 5: Interior of Warehouse 12, image © forensic architecture

Based on a leaked forensic report discussed in [1], the following materials were present in Warehouse 12: ammonium nitrate (2750 tons), fireworks (23 tons), ammonium phosphate (50 tons), coffee and tea (5 tons), detonating cords (5 rolls), 1,000 car tyres, 100 bicycle tyres, slow fuse containing black gun powder used in military and civilian (quarries and crushers) explosives, spare parts for fuel tanks motorcycles, engine working on mazut, pesticides, cow feed, cupboards, bamboo wood, and timber pallets. Using

images leaked from the interior of the warehouse in January 2020, Forensic Architecture mapped the layout of a selection of the goods inside the warehouse including the ammonium nitrate, tyres, fireworks, containers, and wood, as depicted in Figure 5. While this information provides insights to the types of materials that may have been present during the incident, it does not provide a conclusive distribution of materials within the warehouse and was therefore disregarded in Kindling's analysis.

5 Brief introduction to fire dynamics

This section provides an overview of some basic fire dynamic concepts needed to understand the work discussed in subsequent sections. The field of fire dynamics is broad and complex, and thus for further information the reader is referred *An Introduction to Fire Dynamics* by Dougal Drysdale [2].

5.1 Modes of heat transfer

There are three modes of heat transfer, namely, radiation, conduction, and convection, as depicted in Figure 6, and are briefly described in this subsection.

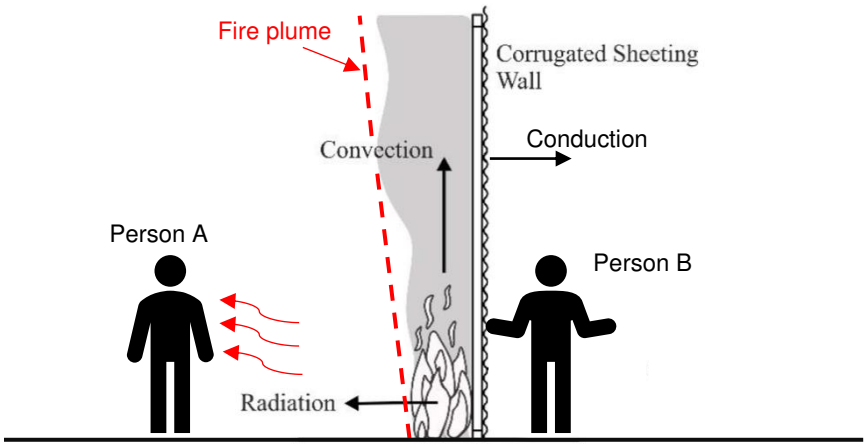

Figure 6: Visual illustration of the different modes of heat transfer (figure reworked from [3]*)*

Radiation refers to the transfer of heat by means of electromagnetic waves and is usually the main mechanism of heat transfer from flames to the surface of combustibles. Considering Figure 6, the heat experienced by person A, on their left side, is a result of radiation.

Conduction refers to heat transfer through a solid material. Considering Figure 6 again, the heat experienced by person B, if they touched the corrugated steel wall, would be a result of conduction through the steel sheets.

Lastly, convection refers to heat transfer by means of fluids (gases or liquids). Convection has a substantial influence on the upward transport of hot gases and smoke to the ceiling

level, typically as a result of upwards buoyancy (an upward force exerted by a fluid that opposes the weight of a partially or fully immersed object) flow. This upwards buoyancy flow is as a result of the heated combustion gases being less dense compared to the surrounding atmosphere. Hence, due to buoyancy the combustion gases will rise along with the fire plume (fire plume is discussed in more detail in Section 5.2). In this work, this upwards buoyancy flow is an important concept when determining the most likely regions of fire origin. Convection also contributes towards the transportation of hot gases and smoke through openings of an enclosure.

5.2 Buoyant plume

A fire plume can be defined as the hot gas flow above and within the flame source [4]. In other words, a fire plume is the buoyant gas flow accompanied by any flames above the flame source [5]. A fire plume consists of three basic regions, namely persistent flame region, intermittent flame region and the buoyant plume region, as depicted in Figure 7.

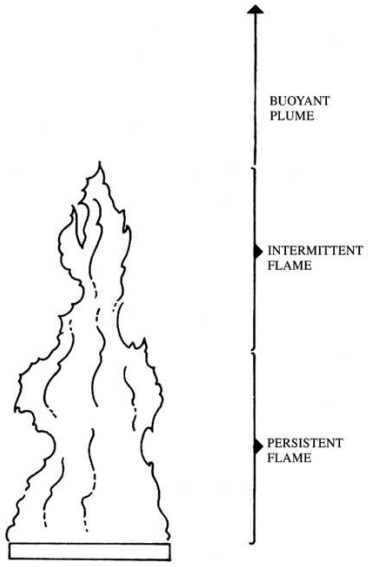

Figure 7: Schematic diagram of the fire plume showing McCaffrey's three regimes [2]

The term 'buoyant plume' is used to describe the convective column rising above a source of heat [2].

6 Methodology

In this work, the Fire Dynamics Simulator (FDS) [6], which is a CFD software with prominence given to fire-driven fluid flow, along with video footage of the actual incident are used to analyse the more probable region of fire origin between two specified scenarios, i.e., scenarios P1 and P2 (Figure 3) as described in Section 1. FDS is

accompanied by an additional program called Smokeview [7], that is used to visually present the FDS predictions.

It is not possible to determine the exact location of fire origin and to reconstruct the ignition sequence with the information available. But the approximate region of fire origin between the two locations of interest can be estimated by utilising FDS modelling and comparing the shape, behaviour, and location of the simulated smoke plume to that of the actual smoke plume captured by videos. Using deductive reasoning, the numerical scenario that best represents the real scenario can be identified; and would then provide information pertaining to the region of fire origin. This is a similar way of reasoning compared to using fire patterns, as discussed in NFPA 921 (international recognized standard for fire investigations) [8], when determining fire origins of building fires.

In this section, a brief discussion on how smoke moves (Section 6.1.) is given as a basis for the methodology described in Section 6.2 and Section 6.3.

6.1 Understanding the movement of smoke (hot gases)

Smoke (and other combustion gases) will move under the influence of forces that are created as a result of a pressure difference or pressure gradient between the smoke and its surrounding. Forces that can move smoke within a building, or in this case within and outside Warehouse 12, can be created by [2]:

a) buoyancy created directly by the fire (Section 5.2);
b) buoyancy arising as a result of a temperature difference between the inside and outside of the warehouse;
c) effects of external wind; and
d) effects of an air handling system within the warehouse.

In this case, points a) and c) are particularly important to determine the most likely region of fire origin between scenario P1 and P2 (Figure 3). It should be noted that the warehouse did not have an air handling system and hence the temperature difference between inside and outside was assumed to be very similar. Thus, the influence of point b) and d) are negligible in this case compared to the thermal influences of a) and c), hence points b) and d) are not considered in this case. Let us consider point c) first, by considering Figure 8.

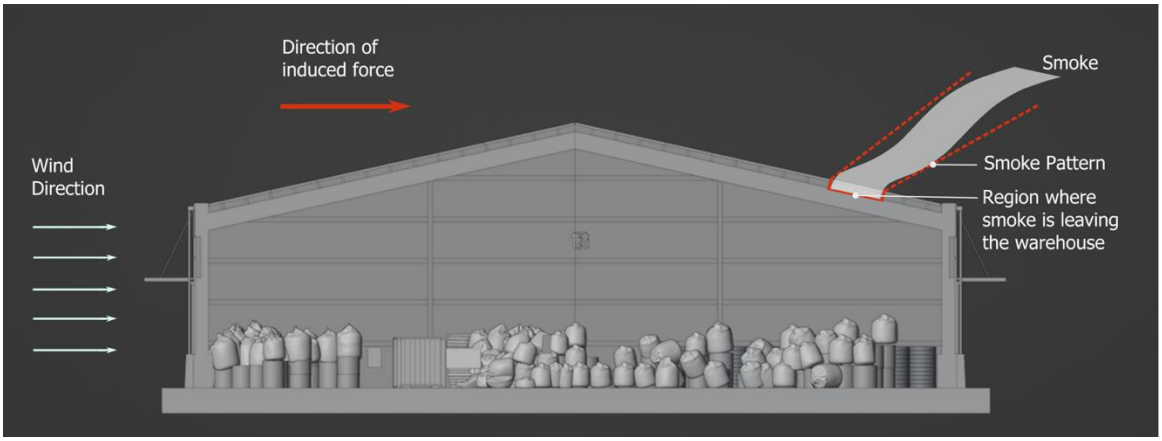

Figure 8: Smoke movement as an effect of external wind

Once the smoke leaves the warehouse, the smoke flows in the same direction as the prevailing wind, which is from southwest to northeast in this case, as depicted in Figure 8). If no wind was present, one would have expected the smoke plume to simply rise upwards, i.e., due to buoyancy.

Using the boundaries of the smoke plume as lines of demarcation between the plume and the environment, it is possible to trace the 'lines of demarcation' between the plume and the environment back to the area where the smoke left the warehouse, as depicted in Figure 8. This is denoted as the 'smoke pattern' in Figure 8.

Point a), i.e., buoyancy created directly by the fire, is visually depicted in Figure 9. Due to the heat of the fire and the lower density of heated combustion gases, e.g. smoke (denoted as smoke throughout for simplicity), compared to the surrounding atmosphere, the smoke will move with the fire plume and rise to the top of the enclosure (or in this case the warehouse), as shown in Figure 9 scenario A. The smoke will continue to rise until it reached the ceiling of the enclosure (Figure 9 scenario B), at which point the smoke will start to move along the bottom of the ceiling (Figure 9 scenario C). It should be noted, that the further away the smoke spreads from the fire source the more air entrainment (i.e., air entrained from the surrounding atmosphere) will occur, implying the gases closer to the fire source would be hotter (e.g., heated area 1 as depicted in Figure 9 scenario C) compared to those further away from the fire source (e.g., heated area 2 as depicted in Figure 9 scenario C).

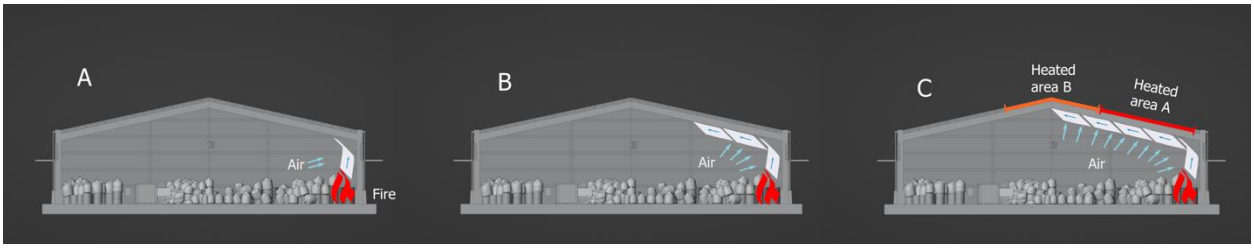

Figure 9: Smoke movement due to the buoyancy created directly by the fire

This analysis is based on the assumption that there were no openings in the roof prior to the fire, and that the fire caused the opening of the roof vents, thus allowing smoke to escape. This assumption appears to be reasonable based on Kindling's review of the warehouse images before the incident, provided by Forensic Architecture.

Hence, if one assumes a scenario where the roof has vents made from plastic sheets, that melt at 170 °C (i.e., within a wide range of the melting temperatures of various plastics [9]), one expects the vents in heated area A to melt before the vents in heated area B as depicted in Figure 9 scenario C. However, it should be further noted here that the slope of the roof might impact the smoke movement, e.g., for a duo-pitched roof, the hot gases will accumulate at the apex of the roof, causing the temperature to rise and potentially offsetting the area where vents would melt first towards the apex. This is investigated in more detail in Section 7 with the use FDS scenarios.

In subsequent subsections, the following analyses are presented:

a) Video analysis of the melted vents (Figure 13),

b) FDS analyses of the open vents (Figure 20 and Figure 22),

c) Video analysis of the smoke plume (Figure 10), and

d) FDS analyses of the smoke plume (Figure 23 and Figure 24).

6.2 Determining the region of fire origin - video analysis

To determine the most likely region of fire origin between scenarios P1 and P2 (Figure 3), the following steps were followed:

a) Using the videos available of the incident, the sequence at which the plastic roof vents opened (i.e., melted) were mapped by Forensic Architecture (Figure 11 and Figure 12) at various time steps as open, closed, and nonconclusive (those that could not be verified as open or closed). A vent was marked as open if smoke was seen leaving the vent.
b) Using the mapped roof vents, the most likely region of fire origin was identified as the region directly below the open mapped vents, i.e., due to buoyancy as discussed in Section 5.1.
c) The most likely scenario, between scenario P1 and P2, was then proposed by comparing the location of the two scenarios to the location of the region identified in the previous step.

6.3 Determining the region of fire origin - FDS analysis

Following the video analysis, FDS was utilized to further analyze the most probable region of fire origin between the two specified scenarios. The following steps were taken:

a) The FDS scenarios were created using the detailed 3D model previously created by Forensic Architecture [1]. Various burner sizes and other sensitivity analysis was considered, discussed, and simulated in this work.
b) Roof vents for each FDS scenario were mapped, using the same approach as described above in Section 6.2.
c) Lastly, the mapped results of the numerical scenarios P1 and P2 were compared to the mapped roof vents (results from Section 6.2). Additionally, the shape, behaviour, and location of the simulated external smoke plume (for each scenario) was compared to the external smoke plume captured by videos.

7 Video analysis and discussion

The video timeline presented in [1], shows the initial smoke plume leaving the warehouse from the northeast corner (Figure 10), while the vents in the northwest corner were still not melted. This is later followed by flame extension through the roof openings of the northeast corner as depicted in Figure 10. After some time, a second smoke plume (with a different smoke colour) came from the northwest corner, implying that a now present in the northwest corner causing those vents to melt, or a fire was burning for a longer duration in the northeast corner and was now causing the vents in the northwest corner to melt.

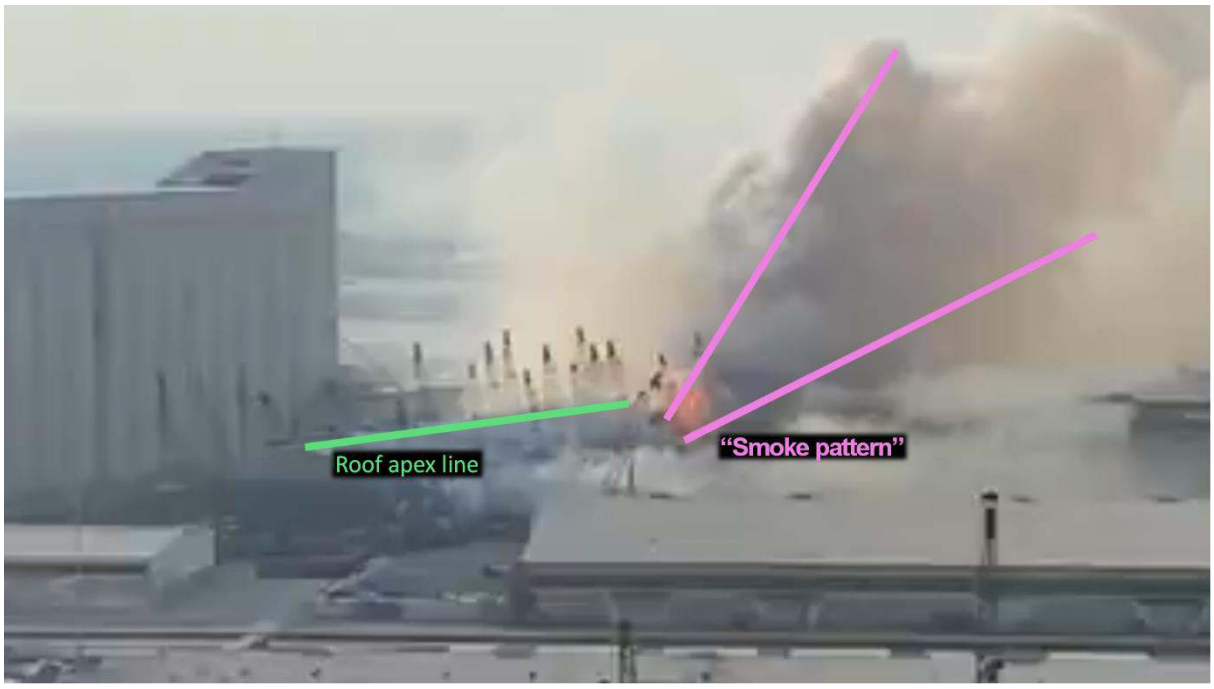

Figure 10: Smoke plume analysis of social media video footage

Using a collection of videos available from various social media sources [1] of the Beirut Port explosion incident, Forensic Architecture created mapped images (Figure 11 and Figure 12) depicting the melted (open), closed, and nonconclusive (i.e., those that could not be verified by Forensic Architecture as open or closed) roof vents.

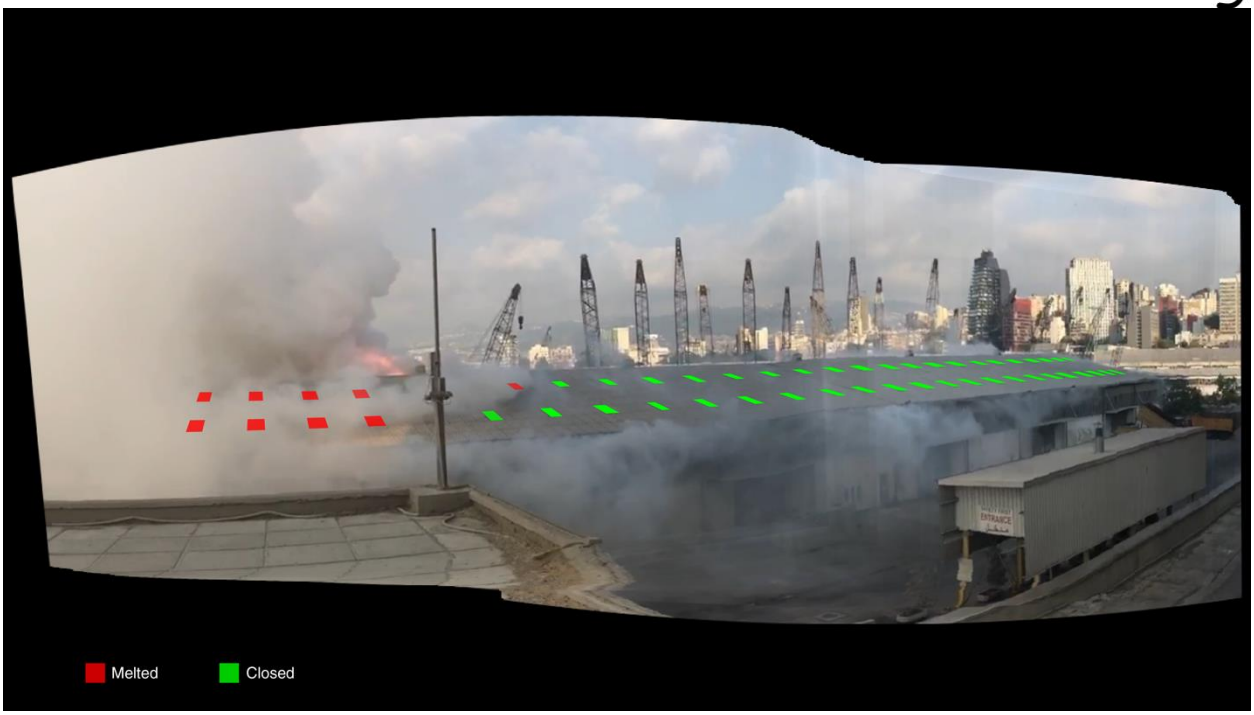

Figure 11: A mapped elevation view image depicting the melted, closed, and nonconclusive (i.e., those that could not be verified as melted or closed) roof vents on the west side of the duo-pitched roof on warehouse 12. As well as the source of the heat plume © forensic architecture

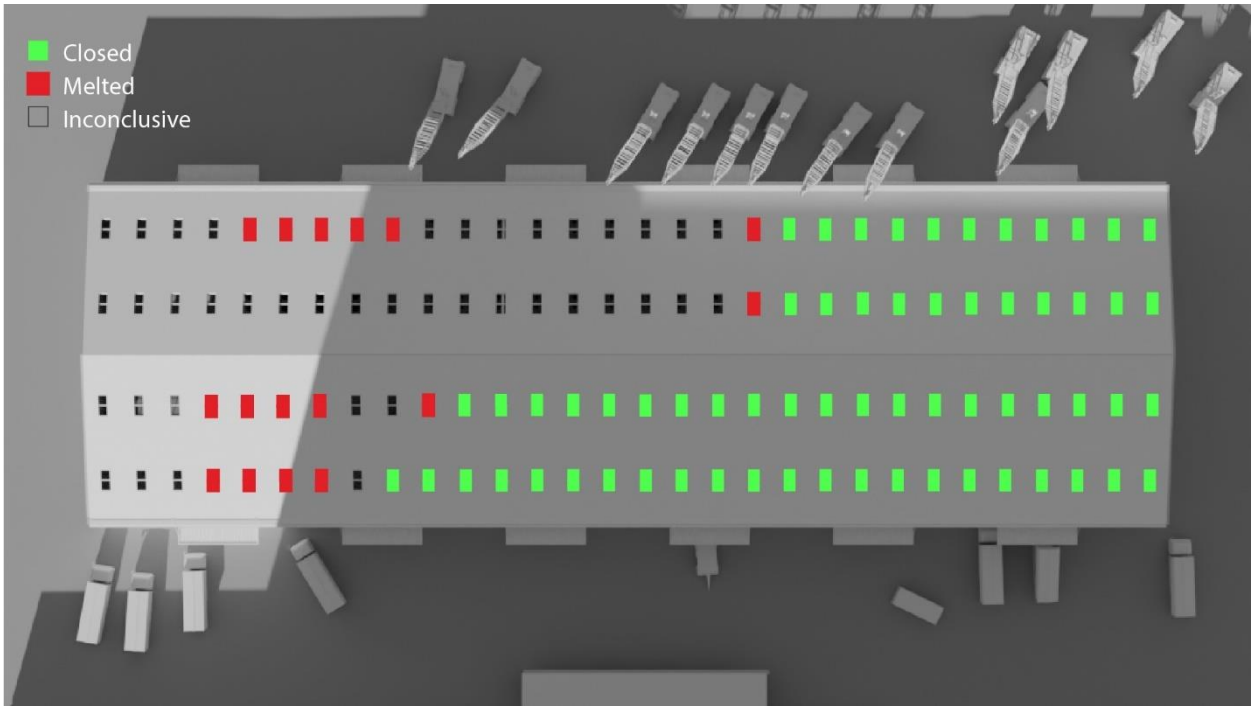

Figure 12: A mapped plan view image depicting the melted, closed, and nonconclusive (i.e., those that could not be verified as melted or closed) roof vents. As well as the source of the heat plume © forensic architecture

Considering the location of the melted vents, it is possible to separate the vents into two distinct sections, namely: a) vents that melted due to hot gases spreading along the length

(north to south) of the warehouse, and b) vents that melted due to hot gases spreading along the width (east to west) of the warehouse, as depicted in Figure 13. Based on the above, it is thus more likely that the fire originated at floor level where these two sections overlap, i.e., in the northeast corner (top-left in Figure 13) inside the blue box shown in Figure 13. There might be a scenario, given the right fuel distribution and ventilation conditions, where the fire could have originated in the northwest corner, however, based on the current information available this appears to be less likely.

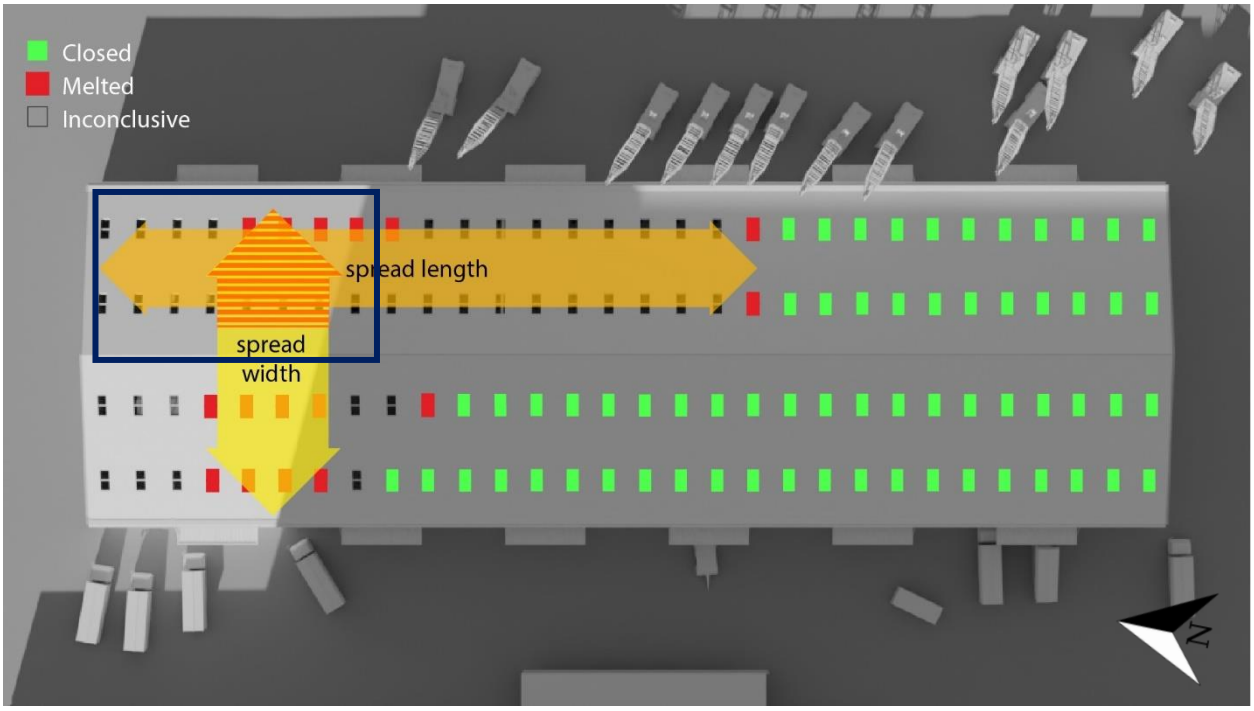

Figure 13: Horizontal fire spread patterns point to the most likely region of fire origin

8 FDS analysis

This section is divided into two subsections, namely: a) FDS set-up, where information pertaining to the warehouse (e.g., geometry, cell size, material properties), wind conditions and fire scenarios used are provided in more detail for each numerical scenario, and b) FDS results, where the results of the various scenarios are discussed and compared to the video analysis results described in Section 7. This section is more technical in nature, and the reader is referred to resources from the developers of FDS for relevant background on this modelling software [6].

8.1 FDS set-up

The 3D model of Warehouse 12 created by Forensic Architecture, was exported as a .fbx file and imported into PyroSim [10] (i.e., a user interface for FDS). In order to incorporate wind in the simulations, the domain boundaries were offset by a minimum of 5H, where

H is the height of Warehouse 12 (14 m), from all faces of the building, as depicted in Figure 14, as proposed by *Wind and Fire Coupled Modelling – Part 2: Good Practice Guidelines* [11]. All domain boundaries were set to open except for z minimum (ground level) which was left as the default inert surface.

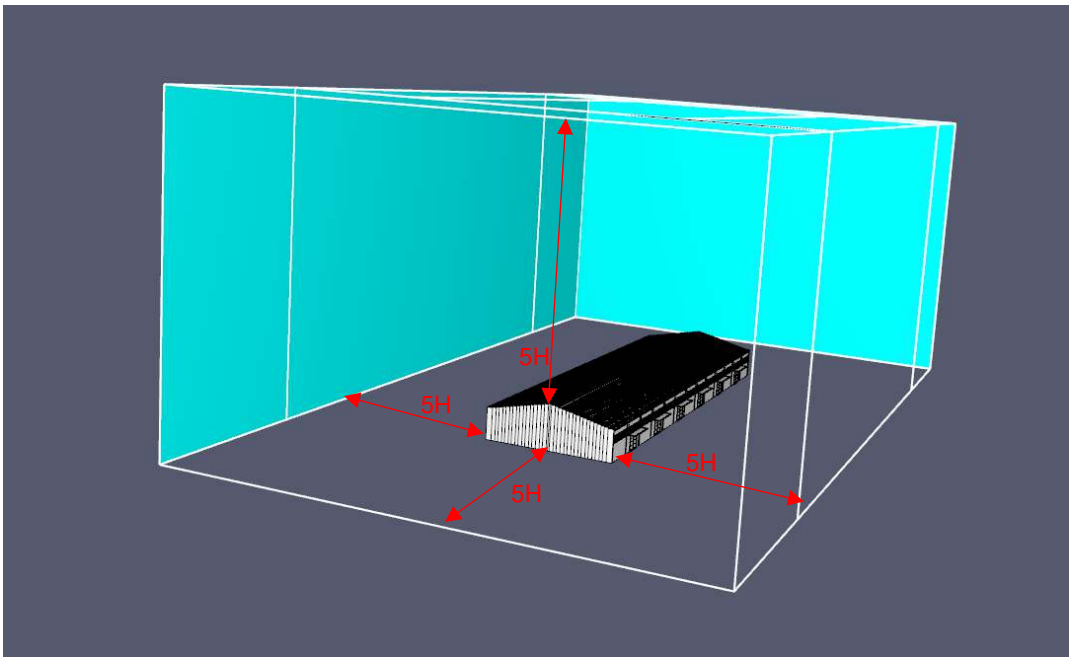

Figure 14: Domain details used in FDS

The cell size of the domain enclosing Warehouse 12 was set to 0.25m and the cell sizes gradually increased (with a factor of two) to a size of 1m for the outer sections of the domain. The cell size enclosing the warehouse was significantly less than the proposed $D^*/_{10}$ value suggested by the FDS validation guide [12], which is based on an approximate method for determining the maximum cell size in FDS simulations [12]. This resulted in approximately 13 million cells. The FDS scenarios were submitted to the High-Performance Computer (HPC) of Stellenbosch University, known as Rhasatsha (https://www0.sun.ac.za/hpc). Rhasatsha currently consists of 2344 cores and each scenario was divided in 23 meshes and each mesh assigned to a core for processing. Each scenario ran for one month and reached approximately 100-150 seconds of simulation time.

The exact size of the fire is unknown but based on a sensitivity analysis it is hypothesized that the size of the fire would not significantly influence the sequence in which the roof vents would have melted. Three scenarios were simulated for each location (P1 and P2) to simulate three different fire sizes in order to test this hypothesis. The various FDS scenarios with fire locations and burner sizes (burners are numerical tools used to simulate the size and heat release rate per unit area (HRRPUA) of a fire in FDS) are listed in Table 3. A HRRPUA of 1000 kW/m^2 was used based on the recommended value range proposed by [13] for storage occupancies. Note the HRRPUA was kept constant, since

the sensitivity of the total heat release rate (HRR), i.e., the total fire size, was analyzed using different burner sizes.

Table 3: Summary of the scenarios simulated in FDS

Scenario denotation	Fire location	Fire area
Scenario P1_1	P1	10x10m
Scenario P1_2	P1	6x6m
Scenario P1_3	P1	2x2m
Scenario P2_1	P2	10x10m
Scenario P2_2	P2	6x6m
Scenario P2_3	P2	2x2m

Custodial functions (i.e., a function which triggers an event, e.g., roof opening when a certain criterion is measured) were used to open the roof vents at an average cell temperature of 170°C. All roof vents were modelled with a gas temperature sampling device that recorded the average temperature of the cell located at the centre of each vent on the inside face of the vent, which then triggered the vents opening.

8.2 FDS results and discussion

Figure 15, Figure 16 and Figure 17 depict the top view of Warehouse 12 with the 3D temperature slice file results for scenario P1_1 to P1_3, respectively. Note that the colour temperature values (i.e., the exact temperature associated with the different colours) are not the same for all scenarios. The temperature values were chosen to show temperature differential for each scenario more clearly. The red indicates the hottest gases for all scenarios and the blue indicates the lowest gas temperature for all scenarios. The exact temperature is not critical to test the hypothesis that fire size does not significantly affect the ventilation opening sequence, but rather the temperature of one region relative to another. To illustrate this, scenarios P1_1 to P1_3 is shown. It should be noted that the same scenarios were modelled for P2_1 to P2_3, which resulted in the same conclusion.

Considering the lack of data on fuel type and distribution with the warehouse, three generalized fire loading conditions were modelled to assess the influence of fire size. A large 10 x 10m fire is shown in Figure 15. A medium 6 x 6m fire is shown Figure 16. A smaller 2 x 2m fire shown in Figure 17. Comparing the open vents between Figure 15, Figure 16 and Figure 17, it is clear that the fire size (total HRR) has a negligible effect on the region that the roof vents melted. Even though the colour temperature values are different, the hottest regions fall within the blue box. This is further illustrated in Figure 18 where the hottest regions for scenario P1_1 versus P1_3 are shown in a section box view across the width of Warehouse 12.

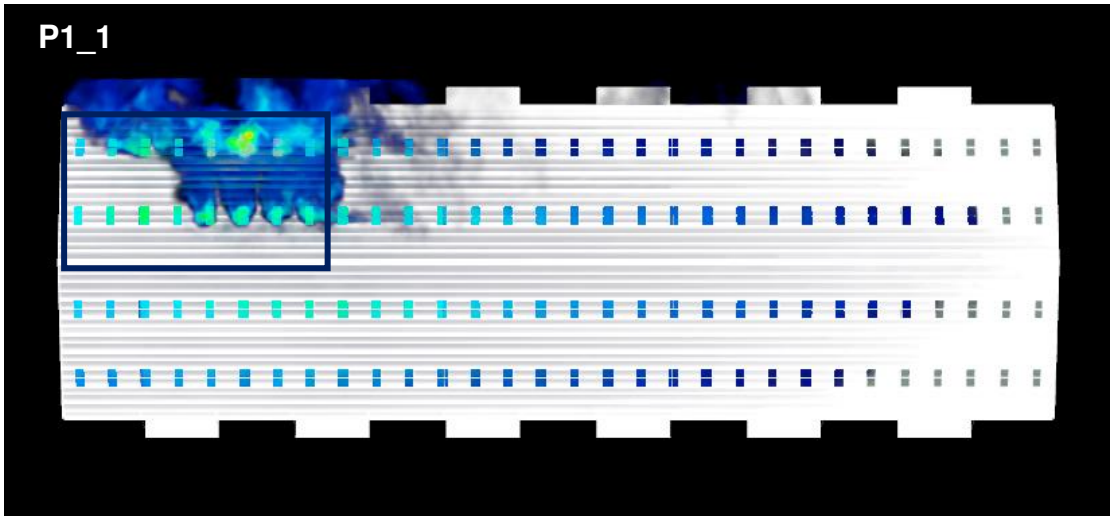

Figure 15: Plan view of Scenario P1_1 showing the 3D temperature slice result. The colour blue indicates coldest regions, red indicates the hottest and green the intermediate region.

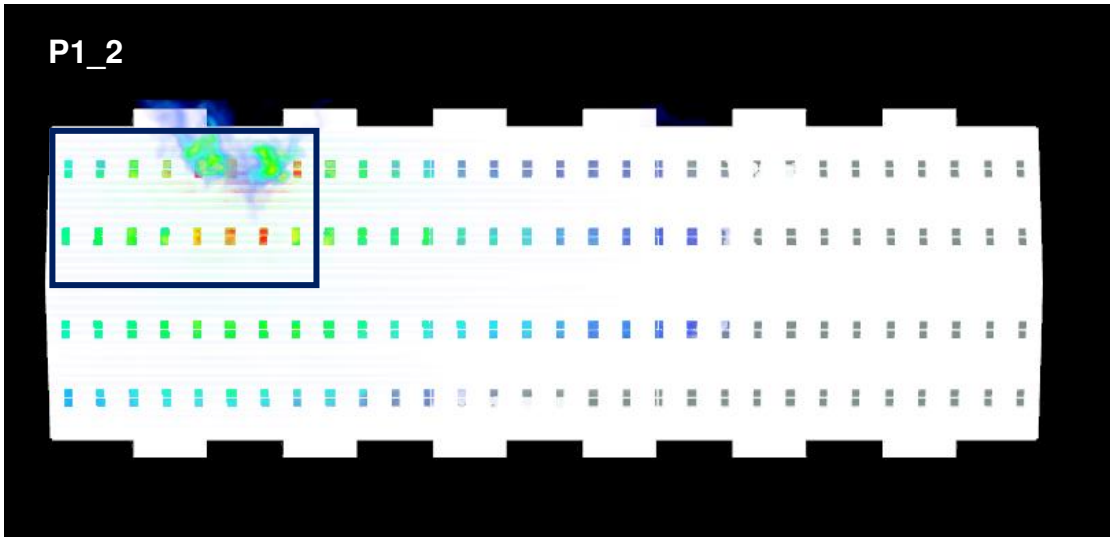

Figure 16: Plan view of Scenario P1_2 showing the 3D temperature slice result. The colour blue indicates coldest regions, red indicates the hottest and green the intermediate region.

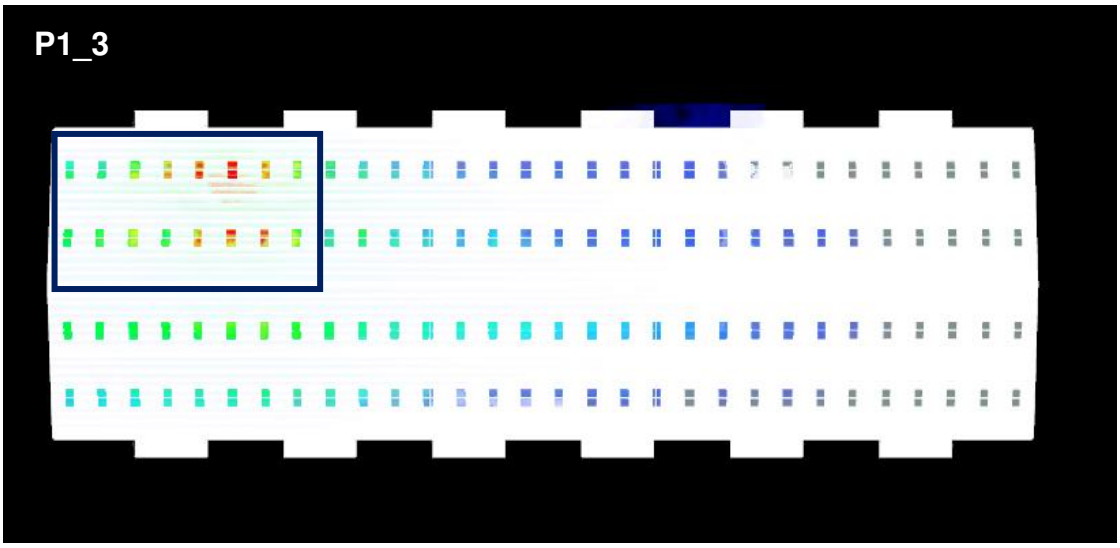

Figure 17: Plan view of Scenario P1_3 showing the 3D temperature slice result. The colour blue indicates coldest regions, red indicates the hottest and green the intermediate region.

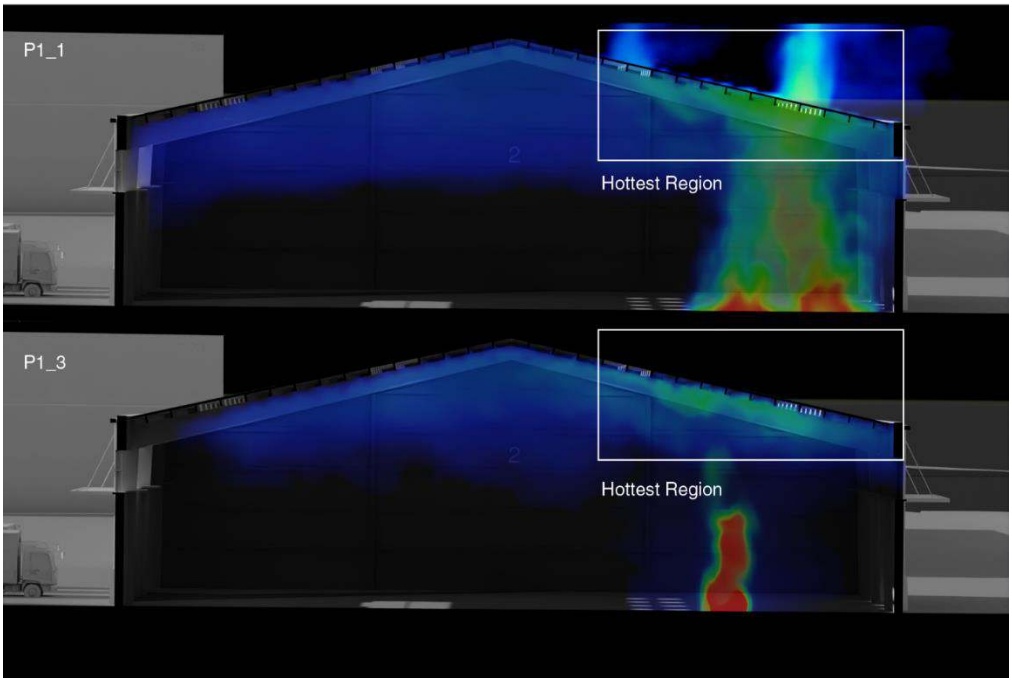

Figure 18: Section box view for scenario P1_1 (top image) and P1_3 (bottom image) across width of Warehouse 12.

Figure 19 depicts the smoke leaving Warehouse 12 for scenario P1_1. Figure 20 depicts the vents that opened (yellow region) during scenario P1_1, along with the open, closed, and nonconclusive roof vents, as shown in Figure 12, obtained from the video analysis of the actual incident. The blue box in Figure 20 depicts the most likely region of fire origin determined in Section 7 using publicly available videos of the incident. Comparing the FDS results (yellow region) to the results obtained in Section 7 (blue box), it is clear that the open vents of the numerical scenario (yellow) correlate well with those identified in the video analysis (blue box).

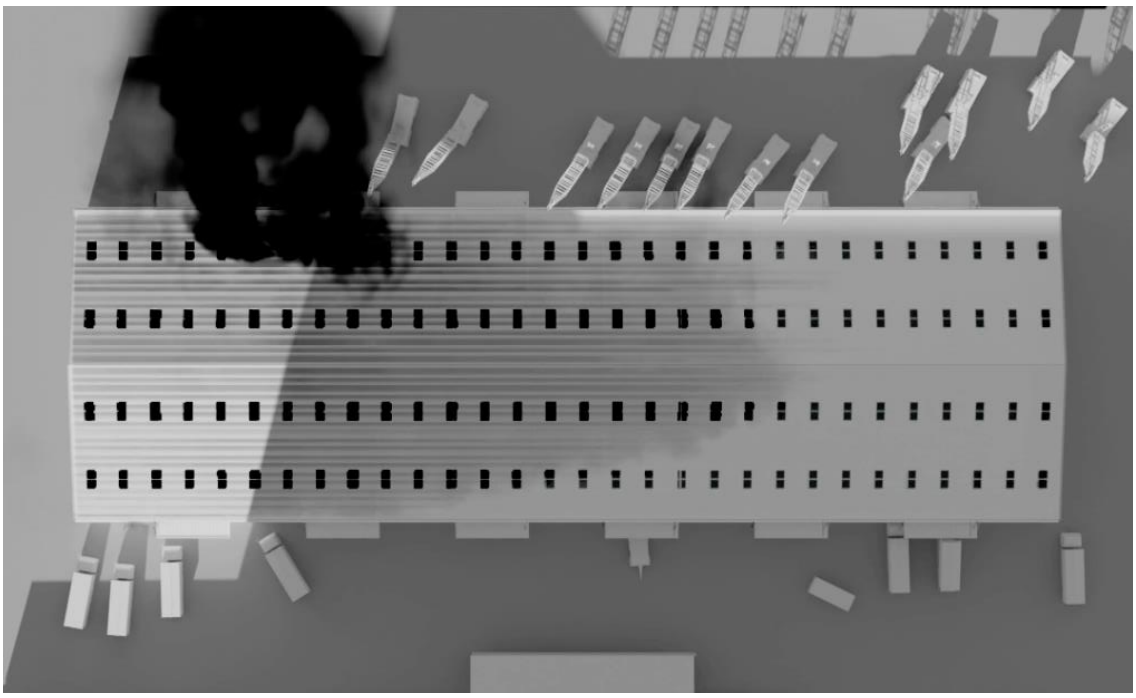

Figure 19: Smokeview image of smoke leaving Warehouse 12 for scenario P1_1.

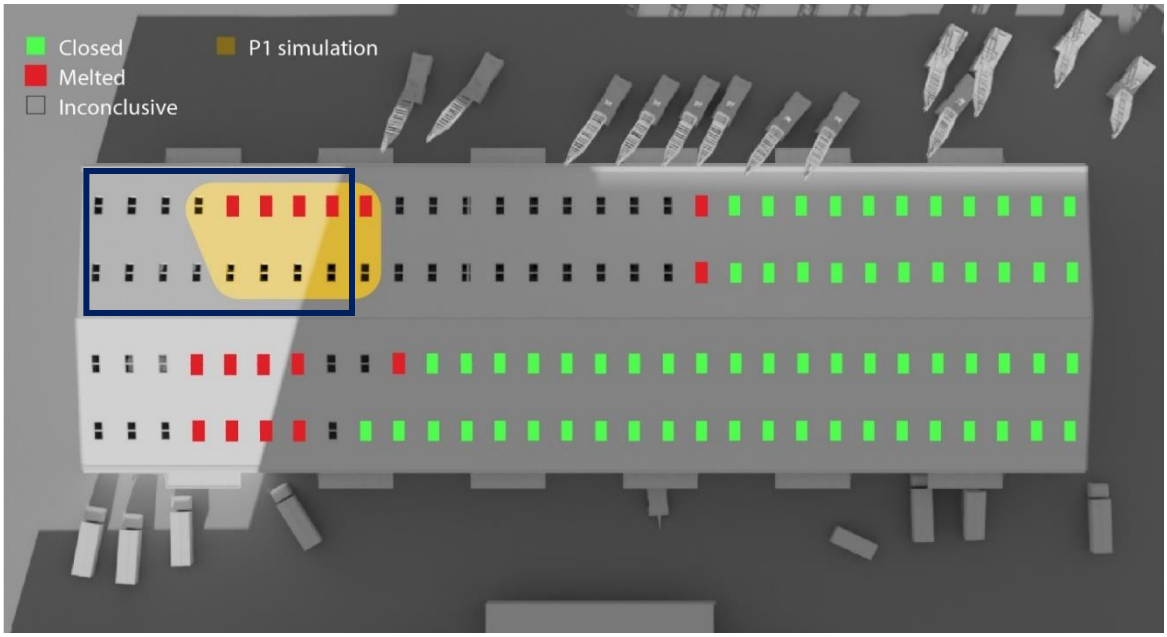

Figure 20: A mapped image depicting the open FDS vents for scenario P1_1 (yellow). Additionally, the open, closed, and nonconclusive roof skylights, as shown in Figure 12, of the video analysis are also shown.

Figure 21 depicts the smoke leaving Warehouse 12 for scenario P2_1. Figure 22 depicts the vents that opened (pink region) during the P2_1 simulation, along with the open, closed, and nonconclusive roof vents, as shown in Figure 12, obtained from the video analysis of the actual incident. Based on the ventilation conditions assumed, the assumption that the fuel load was relatively uniformly distributed, and the sequence at

which smoke was leaving the warehouse vents, the blue box in Figure 22 depicts the most likely region of fire origin determined in Section 7 using publicly available videos of the incident. Comparing the FDS results (pink region) to the results obtained in Section 7 (blue box), it is clear that the open vents of this numerical scenario (pink) do not correlate well with those identified in the video analysis (blue box).

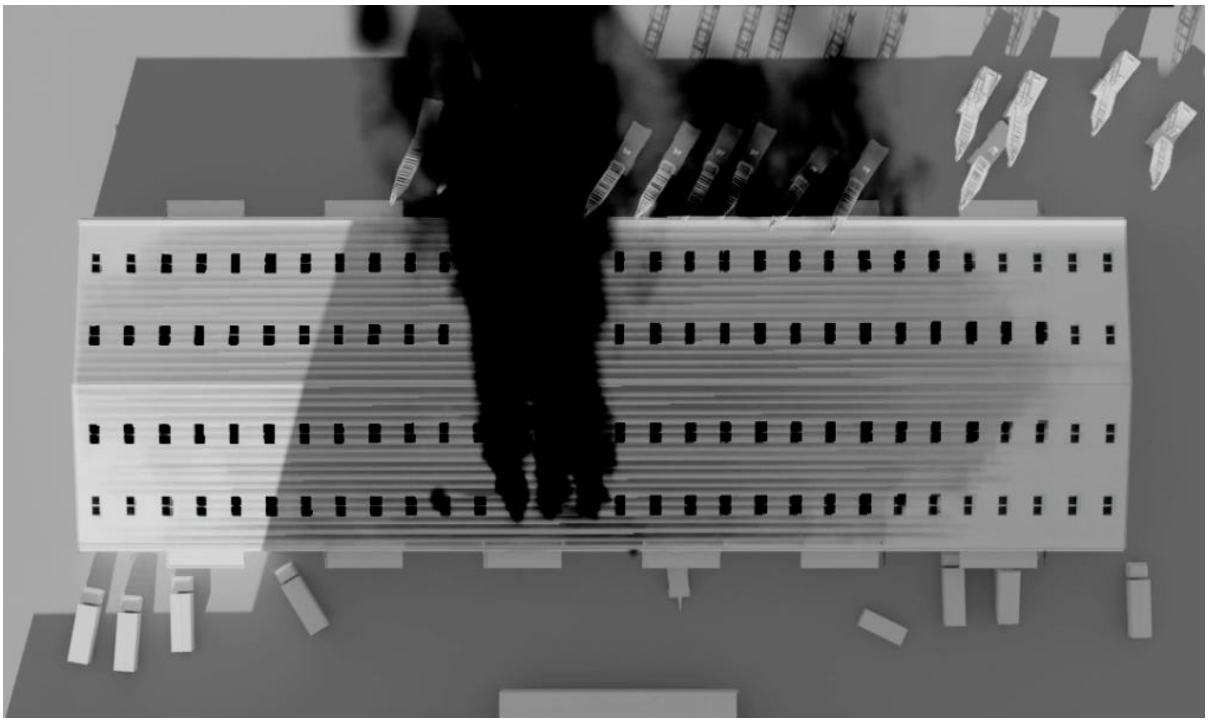

Figure 21: Smokeview image of smoke leaving Warehouse 12 for scenario P2_1.

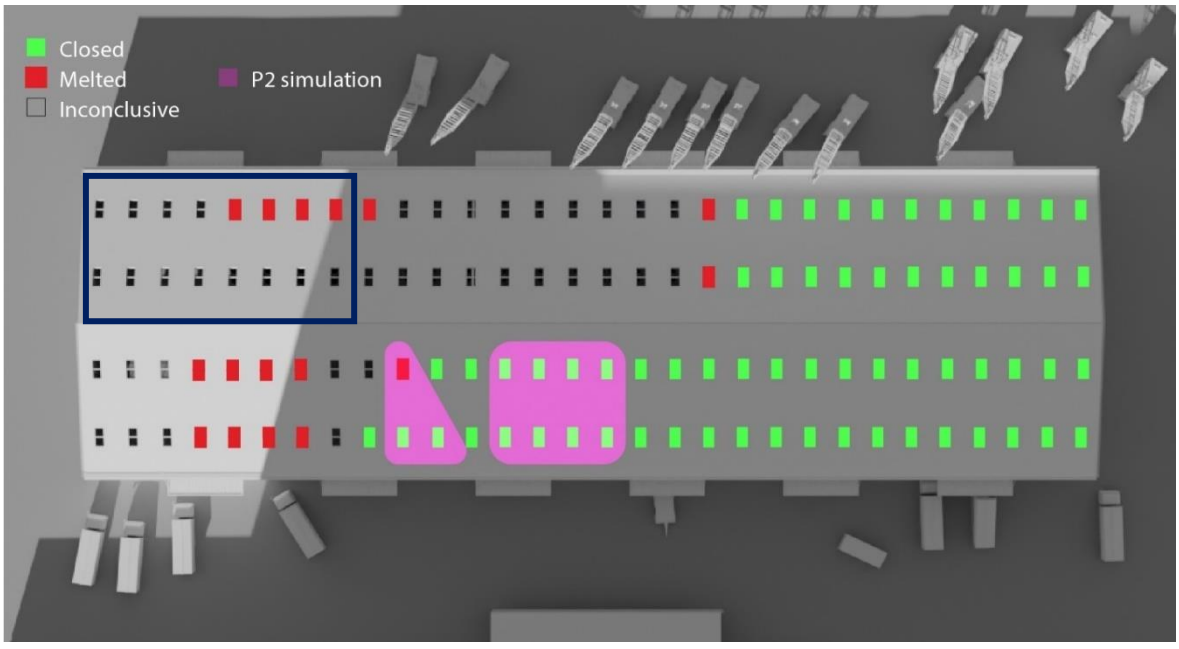

Figure 22: A mapped image depicting the open FDS skylights for scenario P2_1 (Pink). Additionally, the open, closed, and nonconclusive roof vents, as shown in Figure 10, of the video analysis are also shown.

Figure 23 and Figure 24 depict the FDS smoke results for the scenarios P1_1 and P2_1, respectively. A visual 'smoke pattern' analysis has been done for both cases, similar to the analysis described in Section 7 (Figure 10) for the actual incident.

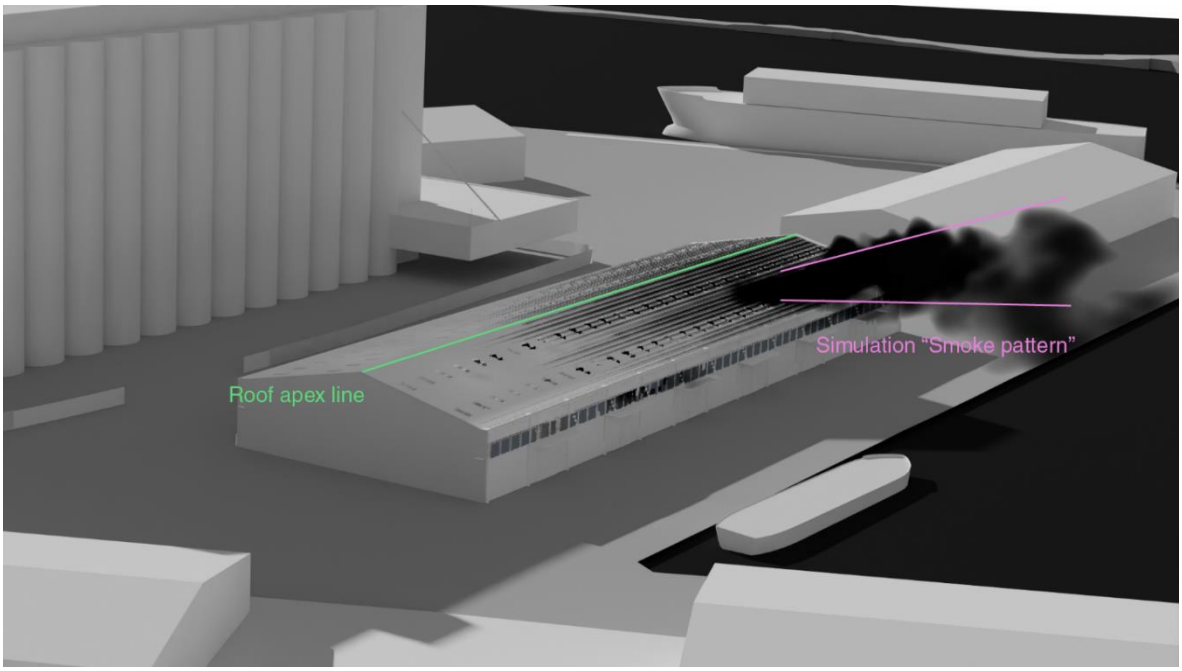

Figure 23: FDS results 'smoke pattern' analysis for scenario P1_1

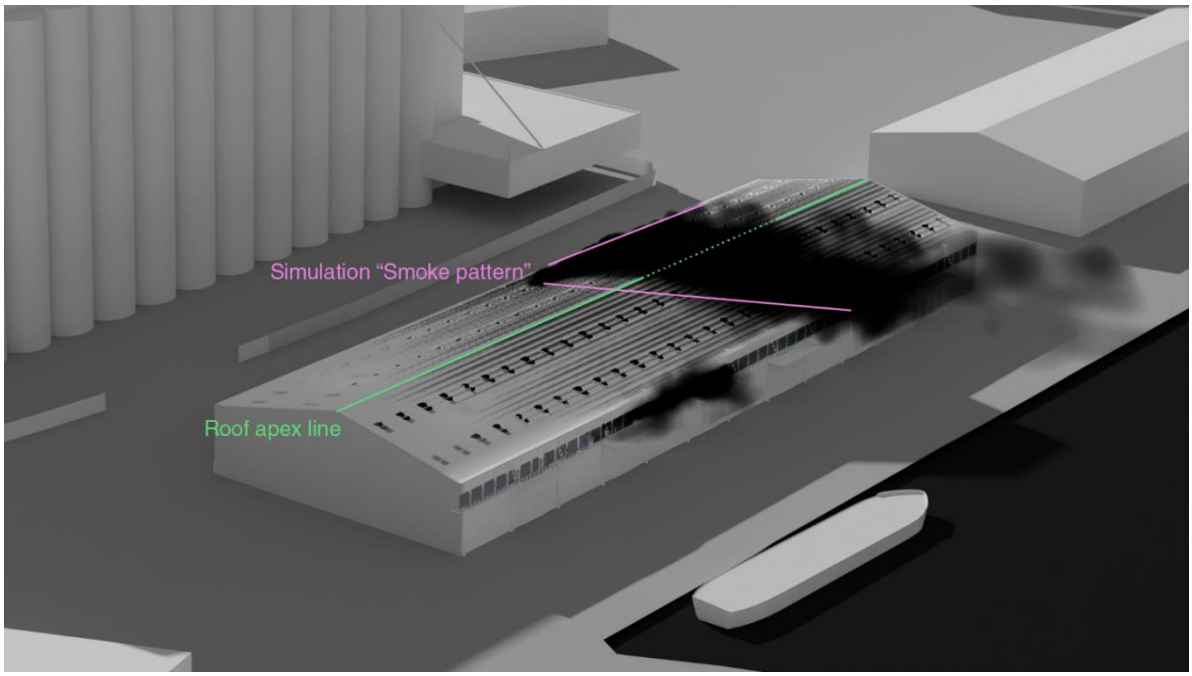

Figure 24: FDS results 'smoke pattern' analysis for scenario P2_1

Comparing the smoke patterns and areas where the smoke leaves Warehouse 12 for scenario P1_1 (Figure 23) and P2_1 (Figure 24) to the actual event (Figure 10) it is clear

that P1_1 and the actual event correlate well, whereas P2_1 and actual event do not correlate well.

Hence, considering the findings from the various simulations and those from the video analysis (Section 7), location P1 (Figure 3) represents the most likely region of fire origin between the two locations provided. This is clear from a) the video analysis of the melted vents (Figure 13), b) the FDS analyses of the open vents (Figure 20 and Figure 22), c) the video analysis of the smoke plume (Figure 10), and d) the FDS analyses of the smoke plume (Figure 23 and Figure 24).

9 Conclusions

As an input to their investigation, Forensic Architecture requested Kindling to carry out an analysis of the warehouse fire that evidently led to the explosion of ammonium nitrate. Forensic Architecture had a very specific question for Kindling to respond to:

Which of the two areas depicted in Figure 3, identified by Forensic Architecture, is the most likely region of fire origin, based on information provided?

- P1, the location previously identified by Forensic Architecture [1] as the source of the smoke plume leaving the warehouse during the early stages of the fire; or
- P2, a new location of interest based on known welding activities that occurred earlier on the day of the incident.

In this report the fire analysis methodology, CFD results, and relevant findings are presented and discussed. The most likely region of fire origin between the two locations in question has been identified as P1, based on the information provided by Forensic Architecture. The main findings are as follow:

- By analysing external smoke plume patterns and the location of melted vents, it was determined that the most likely source of heat was located in the northeast corner of Warehouse 12.
- For the P1 numerical simulations, based on the assumptions made regarding the fuel load and distribution, it was shown that the open vents in the P1 numerical scenarios correlated well with those identified in the video analysis. Whereas, for the P2 numerical simulations, it was clear that the open vents in the numerical scenarios did not correlate well with those identified in the video analysis.
- Comparing the smoke patterns and areas where the smoke left Warehouse 12 for scenario P1 and P2 to the actual event, it is observed that the P1 modelling results correlated well with video evidence of the actual event, whereas P2 scenarios and actual event did not correlate well.

Hence, based on the analyses undertaken in this work, and the information available at the time of the analysis, location P1 is proposed as the most likely region of fire origin between the two regions, P1 and P2, identified by Forensic Architecture.

10 References

[1] The Beirut Port Explosion ← Forensic Architecture, (n.d.). https://forensic-architecture.org/investigation/beirut-port-explosion (accessed June 30, 2022).

[2] D. Drysdale, An Introduction to Fire Dynamics, 3rd ed., John Wiley & Sons, LTD, 2011.

[3] A. Cicione, Fire Dynamics in Informal Settlements, Stellenbosch University, 2019.

[4] B. Karlsson, J.G. Quintiere, Enclosure fire dynamics, CRC Press, London, New York, Washington D.C., 2000. https://doi.org/10.1016/S0379-7112(01)00031-5.

[5] G. Heskestad, Fire Plumes, Flame Height, and Air Entrainment, in: The SFPE Handbook of Fire Protection Engineering, 4th ed., Quincy, MA, USA, 2008: pp. 2–1 to 2–20.

[6] K. McGrattan, S. Hostikka, R. McDermott, J. Floyd, C. Weinschenk, K. Overholt, Fire Dynamics Simulator User's Guide, NIST Special Publication 1019. 6 (2013). https://doi.org/http://dx.doi.org/10.6028/NIST.SP.1019.

[7] G.P. Forney, Smokeview, A Tool for Visualizing Fire Dynamics Simulation Data Volume I: User's Guide, 2018.

[8] National Fire Protection Association, NFPA 921: Guide for fire and explosion investigations, 2017.

[9] V. Babrauskas, Ignition Handbook, 2003.

[10] Thunderhead Engineering, PyroSim User Manual, 2022. https://support.thunderheadeng.com/docs/pyrosim/2020-2/user-manual/ (accessed December 6, 2022).

[11] W. Węgrzyński, T. Lipecki, G. Krajewski, Wind and Fire Coupled Modelling—Part II: Good Practice Guidelines, Fire Technol. 54 (2018) 1443–1485. https://doi.org/10.1007/s10694-018-0749-4.

[12] K. McGrattan, S. Hostikka, R. McDermott, J. Floyd, C. Weinschenk, K. Overholt, Fire Dynamics Simulator Technical Reference Guide. Volume 3: Validation, 3 (2017) 706. https://doi.org/10.6028/NIST.SP.1018-3.

[13] C. Fleischmann, Defining the Heat Release Rate per Unit Area for Use in Fire Safety Engineering Analysis, Fire Science and Technology. (2015) 419–426.